Developmental Cell *10*, 839–850, June, 2006 ©2006 Elsevier Inc. DOI 10.1016/j.devcel.2006.04.002

Dynasore, a Cell-Permeable Inhibitor of Dynamin

Technique

Eric Macia,[1,2,3] Marcelo Ehrlich,[1,2,4] Ramiro Massol,[1] Emmanuel Boucrot,[1] Christian Brunner,[1] and Tomas Kirchhausen[1,*]
[1] Department of Cell Biology
Harvard Medical School and
the CBR Institute for Biomedical Research, Inc.
200 Longwood Avenue
Boston, Massachusetts 02115

Summary

Dynamin is essential for clathrin-dependent coated vesicle formation. It is required for membrane budding at a late stage during the transition from a fully formed pit to a pinched-off vesicle. Dynamin may also fulfill other roles during earlier stages of vesicle formation. We have screened about 16,000 small molecules and have identified 1, named here dynasore, that interferes in vitro with the GTPase activity of dynamin1, dynamin2, and Drp1, the mitochondrial dynamin, but not of other small GTPases. Dynasore acts as a potent inhibitor of endocytic pathways known to depend on dynamin by rapidly blocking coated vesicle formation within seconds of dynasore addition. Two types of coated pit intermediates accumulate during dynasore treatment, ∪-shaped, half formed pits and O-shaped, fully formed pits, captured while pinching off. Thus, dynamin acts at two steps during clathrin coat formation; GTP hydrolysis is probably needed at both steps.

Introduction

Dynamin is essential for clathrin-coated vesicle formation in endocytosis, in transport from the trans Golgi network, as well as for ligand uptake through caveolae ([Abazeed et al., 2005; Cao et al., 2005; Damke et al., 1994; Hill et al., 2001; Nabi and Le, 2003]; reviewed by Nichols [2003]). It is a multidomain protein of ~100 kDa and consists of a GTPase module, a lipid binding pleckstrin-homology (PH) domain, a GTPase effector domain (GED), and a proline/arginine-rich C-terminal segment (PRD), which recruits other proteins through their SH3 domains. Of the three mammalian isoforms, dynamin1 and dynamin2 are the best characterized. In addition to participating in the formation of vesicular structures, both interact with actin binding proteins such as cortactin, influence actin-comet formation on macropinosomes, and affect podosome formation and cell spreading.

Despite extensive studies, the molecular mechanism by which dynamin participates in any of these processes is still a matter of debate. Accumulated evidence indicates that it is critical for the pinching and release of a completed clathrin-coated pit from the plasma membrane as it becomes a fully enclosed coated vesicle. Electron microscopic (EM) images of neurons from *Drosophila* expressing shibire^{ts1}, a temperature-sensitive mutant of the only dynamin present in flies, show profiles, when visualized at nonpermissive temperatures, of noncoated pits (presumably after loss of clathrin) linked to the plasma membrane by necks with electron-dense collars attributed to dynamin (Koenig and Ikeda, 1989; Kosaka and Ikeda, 1983). Similar images from nonneuronal tissues show the accumulation of fully formed coated pits lacking a collar around the neck (Kosaka and Ikeda, 1983). Expression in mammalian cells of other dominant-negative mutant forms that bind nucleotides poorly (e.g., dynamin K44A) leads to accumulation of coated pits that remain open to bulky probes such as avidin (Damke et al., 1994, 1995b). EM images of such cells show coated profiles with a variety of shapes. These cells have long invaginations that are decorated at their tips with clathrin, and they contain dynamin along the tubular connection to the plasma membrane (Damke et al., 2001). Because it takes a day or more to establish the phenotype, there is no way to distinguish whether the coated structures are intermediates or aberrant structures.

Pure dynamin spontaneously forms rings and spirals in conditions of low ionic strength, and it decorates microtubules and lipid vesicles with helices of similar dimensions (Stowell et al., 1999; Sweitzer and Hinshaw, 1998; Zhang and Hinshaw, 2001). Any condition leading to oligomerization, self-assembly, or ring formation also leads to stimulation of the dynamin GTPase by intramolecular contact of GTPase and GED (referred to here as the "intrinsic GAP activity") (reviewed by Eccleston et al. [2002]). Moreover, GTP hydrolysis is linked to a conformational change in the rings and spirals (Chen et al., 2004). These and other observations have influenced the various models proposed to explain the role of dynamin in clathrin-coated vesicle fission (reviewed by Kelly [1999], Kirchhausen [1999], McNiven [1998], Sever et al. [2000b], Yang and Cerione [1999], Orth and McNiven [2003], Praefcke et al. [2004], Sever [2002], and Song and Schmid [2003]).

According to some models, dynamin is a mechanochemical enzyme that is directly responsible for pinching off the vesicle; according to others, it is a regulatory protein that recruits the downstream partner(s), which, in turn, drives the fission step. In the mechanochemical models, dynamin assembles as a collar on the neck of a budding pit, and the cooperative conformational change that accompanies GAP-stimulated GTP hydrolysis leads to neck constriction and scission ([Danino et al., 2004]; reviewed by Danino and Hinshaw [2001]). In the regulatory models, dynamin works like other GTPases as a time-limited recruiting agent. The regulatory models come principally from studies on overexpression of dynamin mutants defective in self-assembly and/or intrinsic GAP activity (Sever et al., 2000a). From

*Correspondence: kirchhausen@crystal.harvard.edu
[2] These authors contributed equally to this work.
[3] Present address: Institut de Pharmacologie Moleculaire et Cellulaire, Centre National de la Recherche Scientifique-Unite Mixte Recherche 6097, 06560 Valbonne, France.
[4] Present address: Department of Cell Research and Immunology, Tel Aviv University, Tel Aviv, 69978, Israel.

the observation that the point mutants dynR725A (defective in GAP activity) and dynK694A (defective in self-assembly) maintain or even stimulate the rate of endocytic uptake of transferrin, it has been proposed that dynamin-GTP, rather than GTP hydrolysis, facilitates vesicle budding (Sever et al., 2000a). From the effect of overexpression of several point mutants in the GED and GTPase domains, the opposite view has been advanced, postulating that efficient GTP hydrolysis and an associated conformational change are both necessary (Marks et al., 2001).

The lifetime of an assembling coated pit is 1–2 min (Ehrlich et al., 2004). Thus, to enlist powerful analyses made possible by contemporary live-cell imaging methods, we require a new way to switch off dynamin on a comparably short time scale. We therefore designed a high-throughput screen to identify small-molecule inhibitors of dynamin that interfere with its GTPase activity. We report the discovery and use of one such compound, which we call dynasore here. Dynasore does not prevent self-assembly of dynamin under low-ionic strength conditions or its binding to lipids, and it acts in vitro as a noncompetitive inhibitor of dynamin1 and dynamin2. We have used this molecule to capture intermediate states in endocytic clathrin-coated pit formation. To proceed beyond each of the intermediates appears to require GTP hydrolysis. One of these intermediates is at the transition point from a hemisphere (∪-shape) to a completely invaginated vesicle (O-shape). The other is after completion of coat assembly (O-shape), just before the coated vesicle is ready to pinch off from the plasma membrane. These observations indicate that dynamin participates in at least two distinct stages of the formation of clathrin-coated pits.

Results

Screen of a Chemical Library for Inhibitors of the GTPase Activity of Dynamin

We developed a simple colorimetric assay (see Experimental Procedures) to search for small molecules affecting the GTPase activity of full-length dynamin1 (Figure 1A). The screen is based on measuring the changes in light absorbance by the dye malachite green due to release of free phosphate upon hydrolysis of GTP by dynamin. To facilitate the screen, we stimulated the GTPase activity of dynamin1 ~50-fold by including the SH3-containing protein Grb2 (fused to GST) in the reaction (Gout et al., 1993). We screened ~16,000 compounds (part of the Diverset E, Chembridge library) at concentrations of 20–50 μM and identified 34 molecules with inhibitory activity; the active compounds were retested by using a fresh stock and a more quantitative radioactivity-based assay to determine their effects on the extent of GTP hydrolysis (Experimental Procedures). For the studies described below, we selected one, named here dynasore (Figures 1B and 1C), because it did not induce aggregation of the dynamin/GST-Grb2 mixture, and because cells treated for up to 48 hr remained viable, did not undergo drastic changes in shape, and did not detach (Figure S1, see the Supplemental Data available with this article online).

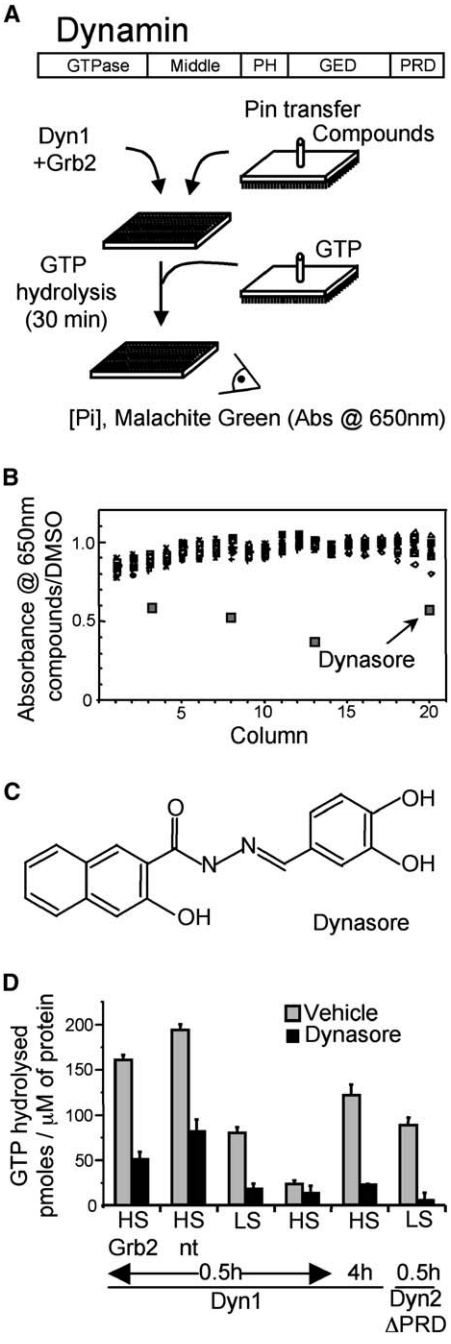

Figure 1. Screen for Inhibitors of Dynamin

(A) Schematic depiction of the domain organization of dynamin and the overall strategy used for the malachite green-based colorimetric screen.

(B) A representative example of data obtained from plate 2 of the primary screen showing four inhibitors of dynamin GTPase activity, including dynasore.

(C) Chemical structure of dynasore.

(D) Effect of dynasore on the GTPase activity of 0.2 μM dynamin1 (Dyn1) or 0.2 μM dynamin2 (Dyn2) lacking its PRD domain (Dyn2ΔPRD) determined under high (150 mM NaCl, HS) or low (15 mM NaCl, LS) salt conditions, with high salt in the presence of 1 μM GST-Grb2 (HS, Grb2) or with high salt together with 100 μM lipid vesicles (HS, nt). The determinations were done after incubation with radiolabeled GTP for the indicated times by measuring the release of $P^{32}O_4$; the values represent the average ± standard deviation from experiments performed in triplicate.

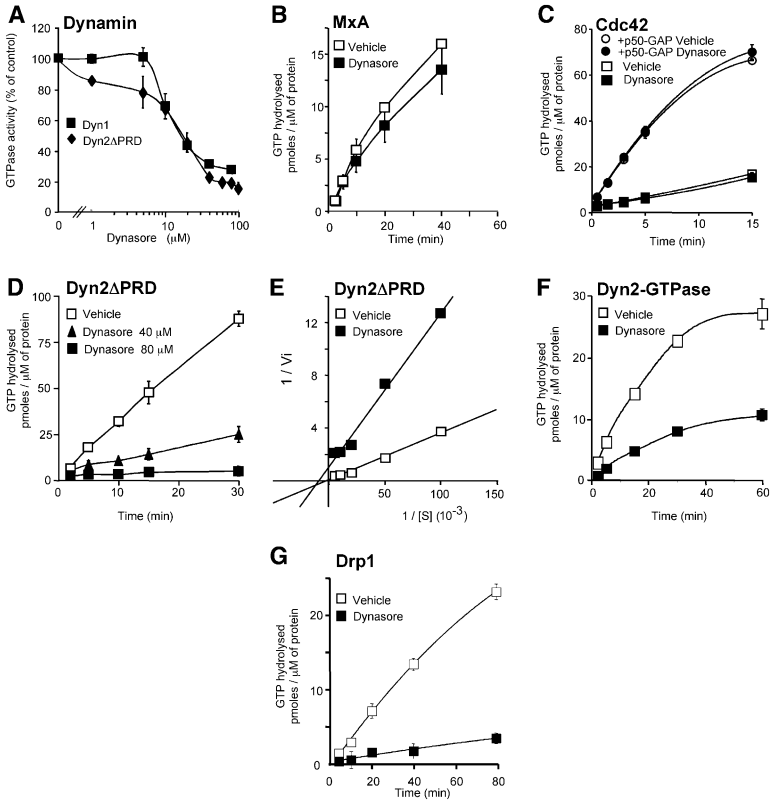

Figure 2. Dynasore Is a Noncompetitive Inhibitor and Acts on the GTPase Domain of Dynamin

The data points represent the average ± standard deviation from experiments performed in duplicate for dose response and in triplicate for kinetics analysis.

(A) Effect of increasing amounts of dynasore on the GTPase activity of 0.2 μM dynamin1 (Dyn1) or 0.2 μM truncated dynamin2 (Dyn2ΔPRD) determined at low salt conditions (15 mM NaCl) and at ambient temperature. The IC_{50} is ~15 μM.

(B) Effect of 80 μM dynasore on the GTPase activity of 2 μM MxA determined at 37ºC. The control experiment was done in the presence of 1% DMSO (vehicle).

(C) Effect of 80 μM dynasore on the GTPase activity of 1 μM GST-Cdc42 determined in the presence or absence of 50 nM p50-GAP at 37ºC. The control experiments were done in the presence of 1% DMSO (vehicle).

(D) Effect of 40 or 80 μM dynasore on the rate of GTPase hydrolysis of 0.2 μM Dyn2ΔPRD determined at ambient temperature. The control experiment was done in the presence of 1% DMSO (vehicle).

(E) Lineweaver-Burk plot showing the noncompetitive effect of dynasore on the GTP hydrolysis of 0.2 μM Dyn2ΔPRD. Rates of GTP hydrolysis were determined at ambient temperature for different concentrations of GTP in the presence (dynasore) or absence (vehicle) of 40 μM dynasore.

(F) Effect of dynasore on the GTPase activity of dynamin2 determined at 37ºC by using 2 μM GST-Dyn2-GTPase domain purified from *E. coli*.

(G) Effect of 80 μM dynasore on the GTPase activity of 2 μM Drp1 determined at room temperature. The control experiment was done in the presence of 1% DMSO (vehicle).

Dynasore Is a Noncompetitive Inhibitor of the GTPase Activity of Dynamin

We confirmed the result from the screen by showing that dynasore inhibits the Grb2-stimulated GTPase activity of dynamin1 at close to physiological salt concentrations (Figure 1D, HS, Grb2). The inhibitory activity does not require the presence of GST-Grb2, as dynasore also interfered with the GTPase activity of dynamin1 stimulated by association with lipid-containing vesicles (Figure 1D, HS, nt) (Stowell et al., 1999). Dynasore also inhibits the GTPase activity of pure dynamin1 stimulated by self-association at low-salt conditions (Figure 1D, LS), as well as its significantly lower intrinsic GTPase activity at physiological salt concentrations (Figure 1D, HS; determined after either a 0.5 hr or 4 hr incubation). In addition, dynasore inhibits the GTPase activity of dynamin2, as stimulated by low-salt-induced self-association and tested by using a truncated dynamin2 that lacks the SH3 binding, C-terminal, proline-rich domain (Dyn2ΔPRD) (Figure 1D, LS, Dyn2ΔPRD). From these results, we conclude that dynasore can inhibit the GTPase activity of dynamin1 and dynamin2 regardless of their assembly state. Because dynasore did not prevent association of GST-Grb2 with dynamin1 in pull-down experiments (not shown), we also propose that dynasore does not interfere with other interactions between either of the dynamins and other SH3 domain-containing partners.

Dynasore inhibits the GTPase activity of full-length dynamin1 or dynamin2 ΔPRD stimulated by self-association (by exposure to low salt) in a dose-dependent manner with a median inhibition concentration (IC_{50}) of ~15 μM (Figure 2A). At 80 μM, dynasore also inhibits the enzymatic activity of the mitochondrial dynamin Drp1 (Figure 2G), but it does not affect the activity of 2 μM MxA (Figure 2B), a subfamily member of the dynamin-like GTPases with antiviral activities (Horisberger, 1992; Kochs et al., 2002), or of the unrelated small GTPase Cdc42, in the presence or absence of its p50-RhoGAP (Lancaster et al., 1994) (Figure 2C). The k_{cat} (2 min^{-1}) and K_m (50 μM) for GTP hydrolysis by dynamin2 ΔPRD (chosen because it is less subject to proteolysis than full-length dynamin) were determined at 25ºC and at low-salt concentrations (Figures 2D and 2E) (Marks et al., 2001; Song et al., 2004). Incubation with 40 μM dynasore (about three times the IC_{50}) had no effect on K_m, but it decreased k_{cat} by about 10-fold (to 0.17 min^{-1}) (Figure 2E). This noncompetitive behavior of dynasore is consistent with interference in the catalytic step rather than in the loading of GTP. Thus, in the presence of inhibiting amounts of dynasore, GTP remains bound to dynamin2 (and by extension to

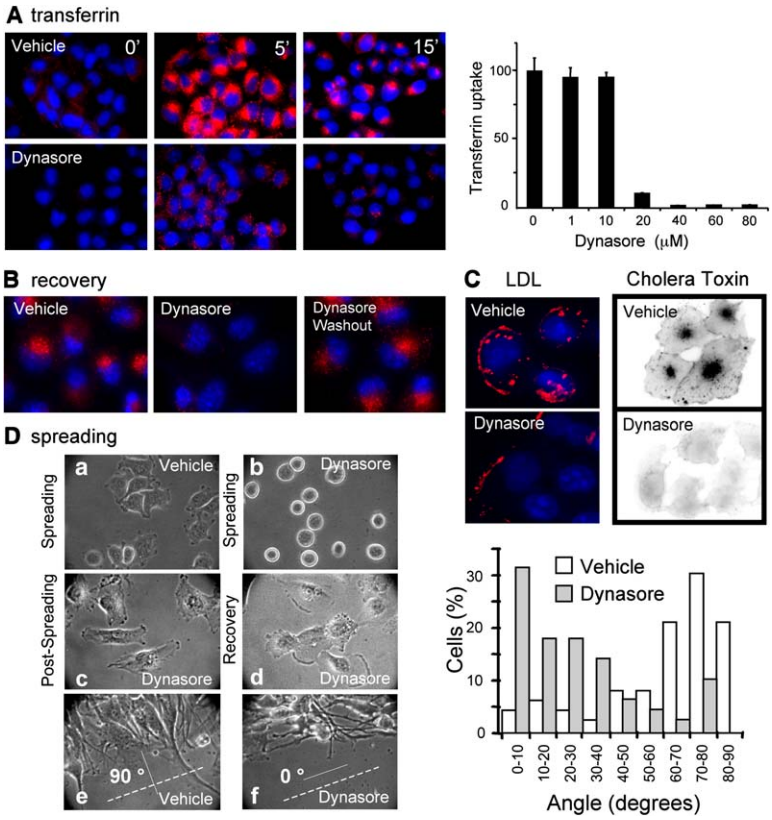

Figure 3. Dynasore Blocks Dynamin-Dependent Internalization of Transferrin, LDL, and Cholera Toxin

(A) HeLa cells were incubated overnight in DMEM supplemented with 5% fetal bovine serum and were allowed to reach 50% confluency. Before addition of transferrin, the cells were incubated for 30 min at 37ºC with 80 μM dynasore or 0.8% DMSO only (vehicle), and then cells were incubated with the same media containing fluorescently labeled Alexa-568 transferrin (red) for 2 min at 20ºC. After three washes with the corresponding media, cells were transferred back to 37ºC and were kept for the indicated times; the cells were acid washed before fixation to remove transferrin still bound at the cell surface. The nucleus is stained with Hoechst dye (blue). The histogram shows the effect of increasing amounts of dynasore on the uptake of transferrin. Internalized Cy3-transferrin was determined as the integrated fluorescence inside 80–100 cells measured for each dynasore concentration.

(B) The inhibitory effect of dynasore on transferrin uptake is reversible. HeLa cells were first treated for 30 min with 0.8% DMSO (vehicle) or 80 μM dynasore (dynasore), followed by treatment in the continuous presence of Cy3-transferrin for 10 min (also at 37ºC), treatment in the presence of DMSO (left), treatment in the presence of 80 μM dynasore (middle), or 20 min after washout of dynasore but still in the presence of DMSO (right). All steps were done at 37ºC.

(C) Effect of dynasore on the uptake of 0.72 μg/ml fluorescently labeled Alexa-647 LDL (red) or 20 nM Alexa-594 cholera toxin (black) in BSC1 cells treated first with 0.8% DMSO (vehicle) or 80 μM dynasore for 30 min. The uptake of LDL or cholera toxin was determined upon continuous incubation of cells for 30 min. The mean fluorescence intensity/cell of internalized LDL was 33.3 ± 7.4 and 10.9 ± 1.2 (n = 50 cells) in cells treated with vehicle or with dynasore, respectively. The total number of LDL receptors was increased by incubating the cells overnight in medium lacking serum before carrying out the experiment. All steps were done at 37ºC. Images are representative of experiments performed in triplicate.

(D) Effect of dynasore on cell spreading. BSC1 cells were suspended by mild trypsinization and were plated back in PBS supplemented with 0.4% glucose in the presence of 0.4% DMSO ([a], vehicle) or 80 μM dynasore/0.4% DMSO ([b], dynasore) for 30 min at 37ºC. BSC1 cells were first plated in the absence of dynasore, and, after 30 min, they were incubated with 80 μM dynasore for another 2 hr at 37ºC ([c], dynasore). Alternatively, cells were first plated in the presence of dynasore as in condition (b), followed by incubation in the absence of dynasore for 16 hr at 37ºC ([d], dynasore), and were allowed to spread in the presence of PBS supplemented with 0.4% glucose. Images are representative of results from experiments carried out in duplicate. The effect of dynasore on the orientation of BSC1 cells was determined by following their spreading toward a scratch applied to a monolayer of cells. The images were obtained 44 hr after the scratch by using cells kept in the presence of DMSO ([e], vehicle) or 80 μM dynasore ([f], dynasore). The experiment was done with PBS supplemented with 0.4% glucose. The orientation is the angle subtended by the longest axis of the cells with respect to the direction of the scratch; 90º represents a perpendicular orientation. The histogram presents the orientation for ~60 cells scored in the presence or absence of dynasore.

dynamin1). We suggest that the GTPase domain contributes an important portion of the protein surface targeted by dynasore, because dynasore also inhibits the hydrolysis of GTP mediated by the isolated GTPase domain of dynamin2 (Figure 2F) or dynamin1 (Figure S2).

Dynasore Interferes with Endocytic Functions that Depend on Dynamin

To establish whether dynasore can act in intact cells, we examined its effect on the uptake of transferrin and LDL. Entry of these ligands is completely dependent on the normal function of dynamin; transferrin and LDL bind at the cell surface to their corresponding receptors, which, in turn, are internalized by receptor-mediated endocytosis, a process that requires the formation of clathrin-coated pits and vesicles (Ehrlich et al., 2004; Hanover et al., 1984). Alexa-568 transferrin was allowed to bind to its receptor on the surface of HeLa cells by incubation for 2 min at 25ºC (to slow down endocytosis; Figure 3A, vehicle, 0 min). Upon warming to 37ºC, the receptor bound Alexa-568 transferrin rapidly internalizes, first trafficking to peripheral early endosomes (5 min) and then to perinuclear-recycling late endosomes (15 min). The uptake, trafficking, and intracellular accumulation of transferrin were all strongly blocked in cells preincubated for 30 min with 80 μM dynasore, which was also present during the uptake assay (Figure 3A, dynasore). The extent of the endocytic block was similar to that observed upon overexpression of dynaminK44A, a mutant form defective in nucleotide binding and hydrolysis (Damke et al., 1994). The inhibition of transferrin uptake is dose dependent (Figure 3A) and has an IC_{50} (~15 μM) very close to the IC_{50} determined in vitro for the inhibition of pure dynamin1 or dynamin2 (Figure 2A). Treatment with similar amounts of dynasore also blocked the transferrin uptake in other cell types such as monkey BSC1 and COS1 cells and human U373-MG astrocytes (not shown). The decrease in transferrin

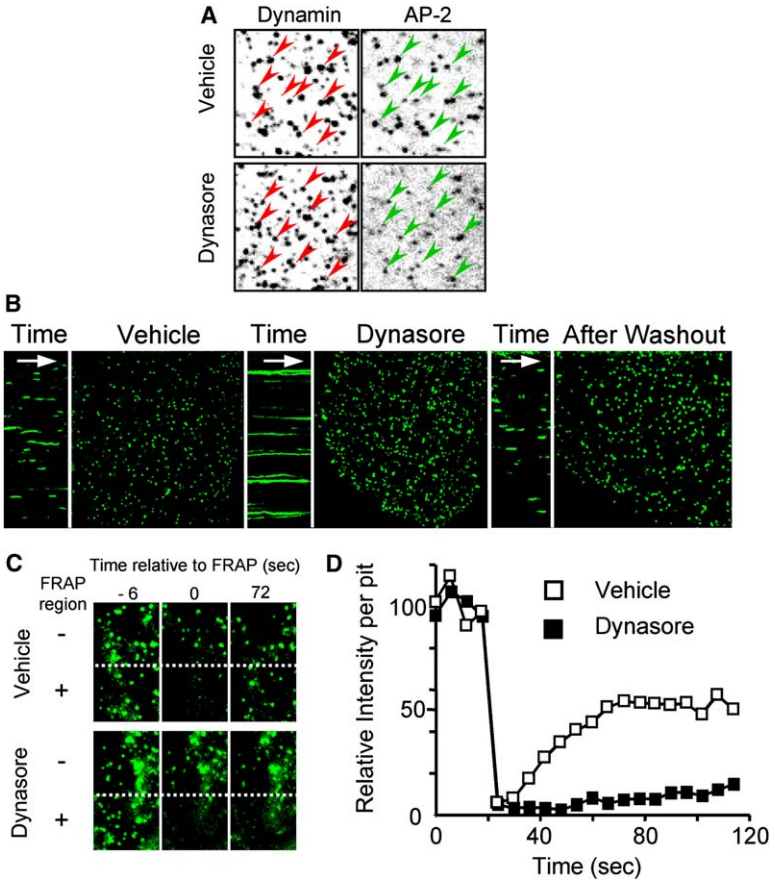

Figure 4. Dynasore Stabilizes AP-2-Containing Coated Structures

(A) Colocalization of dynamin2- and AP-2-containing pits in the presence and absence of dynasore. BSC1 cells stably expressing σ2-adaptin fused to EGFP were used to label the clathrin-coated structures at the plasma membrane containing AP-2; the cells were treated with 0.8% DMSO (vehicle) or 80 μM dynasore (dynasore) at 37ºC for 30 min, fixed, stained with the antibody Hudy-2 (Upstate), which is specific for dynamin2, and then imaged by fluorescence microscopy. Most AP-2 spots contain dynamin, and a similar subset of dynamin spots (red arrowheads) colocalize with AP-2 (green arrowheads) under both conditions.

(B) Live-cell fluorescence imaging acquired from the bottom surface of BSC1 cells stably expressing σ2-EGFP. Time-lapse series were collected for 6 min at 37ºC in the presence or absence of dynasore from cells preincubated for 40 min with either DMSO (vehicle) or 80 μM dynasore (dynasore) or in the absence of dynasore from cells first incubated for 40 min with 80 μM dynasore and then for 20 min with DMSO (after washout). Each still image corresponds to a frame acquired after 3 min of data collection, while the kymographs (time) represents the complete time-lapse series obtained with the spinning disk confocal configuration (1 s exposures, acquired every 4 s). The data are representative of the experiment done in triplicate.

(C) Effect of dynasore on the fluorescence recovery after photobleaching (FRAP) of AP-2-containing spots. BSC1 cells stably expressing σ2-EGFP were subjected to a FRAP protocol, followed by immediate imaging of their bottom surface with the spinning disk confocal configuration. FRAP was done in cells exposed for 40 min to either DMSO (vehicle) or 80 μM dynasore (dynasore). The panels represent images obtained from areas of cells not subjected to bleaching (− FRAP region, negative controls) or from the photobleached area (+ FRAP region) acquired before (−6 s) or after (0, 72 s) photobleaching.

(D) Plot of the integrated fluorescence intensity for all pits shown in (C) as a function of time. The data show recovery of fluorescence intensity specific for the pits (e.g., corrected by the recovery from the surrounding background) and are representative of an experiment done in triplicate.

uptake is not due to a decrease in the number of transferrin receptors, to which transferrin could bind at the cell surface, or to a decrease in the association of transferrin with its receptor, as the amount of surface bound transferrin was the same in cells kept for 30 min at 4ºC in the presence or absence of dynasore (not shown). The effect of dynasore on transferrin uptake is completely reversible, as traffic to perinuclear endosomes returned to normal levels 20 min after the removal of dynasore from the medium (Figure 3B, dynasore washout; compare the endosomal signals of internalized transferrin in the left and right panels). Dynasore also elicits a powerful block in the receptor-mediated endocytosis of LDL, demonstrated here by showing that the internalization and endosomal accumulation of Alexa-546 LDL in HeLa cells (Figure 3C, vehicle) is absent in the presence of dynasore (Figure 3C, dynasore).

Cholera toxin uptake also involves entry routes largely dependent on dynamin activity (Henley et al., 1998; Massol et al., 2004; Oh et al., 1998). A 30 min pretreatment of BSC1 cells with dynasore interferes with the entry and subsequent intracellular accumulation of Alexa-594 cholera toxin in endosomal and Golgi compartments (Figure 3C, dynasore); the extent of this block is similar to that observed upon expression of the dominant-negative mutant dynaminK44A (Massol et al., 2004; Torgersen et al., 2001). Indeed, treatment with dynasore of Y1-adrenal cells used in a functional assay that measures cholera toxin-elicited toxicity by monitoring changes in cell shape did not prevent the cholera toxin effects. These results confirmed our previous observation that blocking the dynamin-dependent endocytic traffic is not sufficient to prevent toxin action (not shown).

Dynasore Inhibits Cell Spreading and Migration

Overnight expression of dynamin2K44A or S45N (both weak binders of GDP and GTP [Damke et al., 2001]) reduces cell spreading, but not cell adhesion (Schlunck et al., 2004), suggesting that spreading requires GTP binding and/or hydrolysis by dynamin. Short treatment (30 min) of BSC1 cells (and astrocytes, not shown) with dynasore strongly interferes with the spread of freshly plated cells (Figure 3D; compare [a] and [b]); extended treatment (2 hr) with dynasore did not led to cell rounding or detachment (Figure 3D, [c], and data not shown for incubations lasting 72 hr). The effects of dynasore on cell spreading are reversible, as removal of dynasore after plating the cells (in the presence of dynasore) led to recovery of normal spreading behavior 16 hr after plating (Figure 3D, [d]). Polarized cell migration and

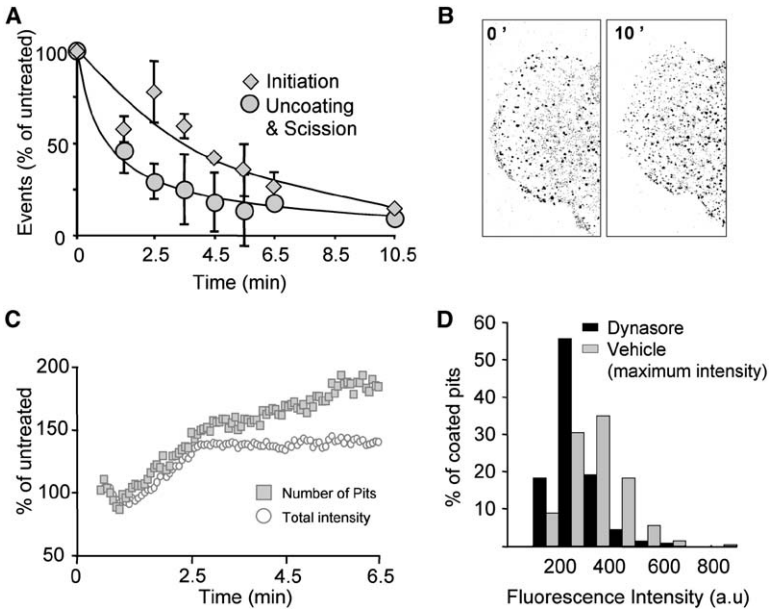

Figure 5. Effect of Dynasore on the Dynamics of AP-2-Containing Coated Structures

BSC1 cells stably expressing σ2-EGFP were imaged by spinning disk confocal microscopy starting 30 s after the addition of 80 μM dynasore.

(A) The plot provides the number of new AP-2 spots appearing (Initiation) and disappearing (Uncoating & Scission) calculated at selected time points. The fate of the disappearing spots refers to those that reached the average maximum intensity of AP-2 fluorescence of coated pits before addition of the compound. The data derive from three cells and are normalized as the percentage of events with respect to the same cells before addition of dynasore. Approximately 200 spots were counted for each condition and each cell, covering an area of 100–200 × 200 pixels (0.1 micron/pixel); images were acquired every 4 s with 1 s exposures.

(B) Representative images from the time-lapse series presented in (A) acquired before or 10 min after the addition of 80 μM dynasore.

(C) Effect of dynasore on the number of AP-2-containing spots and their integrated intensity measured for up to 6.5 min after the addition of 80 μM dynasore. The plot represents the number of σ2-EGFP spots and their total fluorescence intensity as a function of time normalized for their corresponding values in the same cells before dynasore treatment. Data correspond to images obtained from three cells by using the same imaging conditions as in (A).

(D) Effect of dynasore on the distribution of fluorescence intensities of σ2-EGFP-containing spots. The histogram distribution compares the maximum fluorescence intensity of AP-2 spots just prior to their uncoating, determined with a time-lapse series in cells not exposed to dynasore (gray), with the fluorescence intensity reached in the same cell by AP-2 spots after treatment for 10 min with 80 μM dynasore (black); at these points, no new coats form. To prevent photobleaching, no other images were acquired during the 10 min interval. The data were obtained from 4 cells and include 285 and 384 pits in the absence and presence, respectively, of dynasore.

reorientation of the migrating cells toward the edge of a scratch in a monolayer of cells are other processes that require dynamin function; both are prevented in cells overexpressing dynaminK44A (Ezratty et al., 2005). We grew BSC1 cells as a monolayer and then determined the orientation of the cell extensions 44 hr after making the scratch (Figure 3D, [e], [f], and the corresponding histogram). As expected, in the absence of dynasore, most of the cells (70%) extended toward the scratch (Figure 3D, vehicle, >60º); in contrast, less than 20% of the cells showed this behavior when exposed to 80 μM dynasore (Figure 3D, dynasore).

Dynasore Does Not Affect Dynamin-Independent Functions

Biosynthesis of membrane proteins in the endoplasmic reticulum (ER) and trafficking of these proteins to the Golgi apparatus do not require dynamin (Altschuler et al., 1998). Treatment of BSC1 cells with 80 μM dynasore (sufficient to block transferrin uptake completely) had no discernable effect on the efficiency of transferrin receptor biosynthesis or on its subsequent arrival in the Golgi apparatus (Figure S3A), as measured by the acquisition of endoglycosidase H sensitivity (Figure S3A, 20 min) and endoglycosidase H resistance (Figure S3A, 60 min). Moreover, treatment (up to 90 min) of BSC1 cells with 80 μM dynasore had no detectable effects on overall protein synthesis, as determined by the incorporation of S^{35}-labeled methionine into newly synthesized proteins (Figure S3B).

We also tested the effect of dynasore on fluid phase uptake of soluble molecules from the media into cells. Fluid phase uptake is a complex process involving the formation of many types of vesicular and vesiculotubular carriers; only a fraction of this uptake (~50%) is sensitive to inhibition of dynamin function, as shown by transferring cells expressing a temperature-sensitive mutant of dynamin to the nonpermissive temperature of 38ºC (Damke et al., 1995a). A short-term treatment of BSC1 cells with 80 μM dynasore led to a ~60% drop in fluid phase uptake, monitored here by the uptake of soluble horseradish peroxidase (Figure S3C). In HeLa cells incubated with saturating conditions of ligand (>20 ng/ml EGF), the internalization of activated epidermal growth factor receptors is not blocked by expression of dynaminK44A, indicating that under this condition most of the receptor is internalized through a clathrin- and dynamin-independent pathway (Jiang and Sorkin, 2003). In agreement with this observation, the presence of 80 μM dynasore in HeLa cells treated for 10 min with 100 ng/ml EGF had little effect on receptor internalization (Figure S3E). Finally, a 40 min treatment of BSC1 cells with 80 μM dynasore did not alter the intracellular distribution of assembled tubulin or actin (Figure S3D). Taken together, these observations indicate that the cellular effects of dynasore appear to be restricted to dynamin-related functions.

Dynasore Arrests the Formation of Endocytic Clathrin-Coated Pits and Vesicles

Because of the key role of dynamin in clathrin-mediated endocytosis, we chose to study in more detail the effects of dynasore on the formation of clathrin-coated pits and vesicles. Dynamin is recruited to the plasma membrane in a punctate pattern that partially

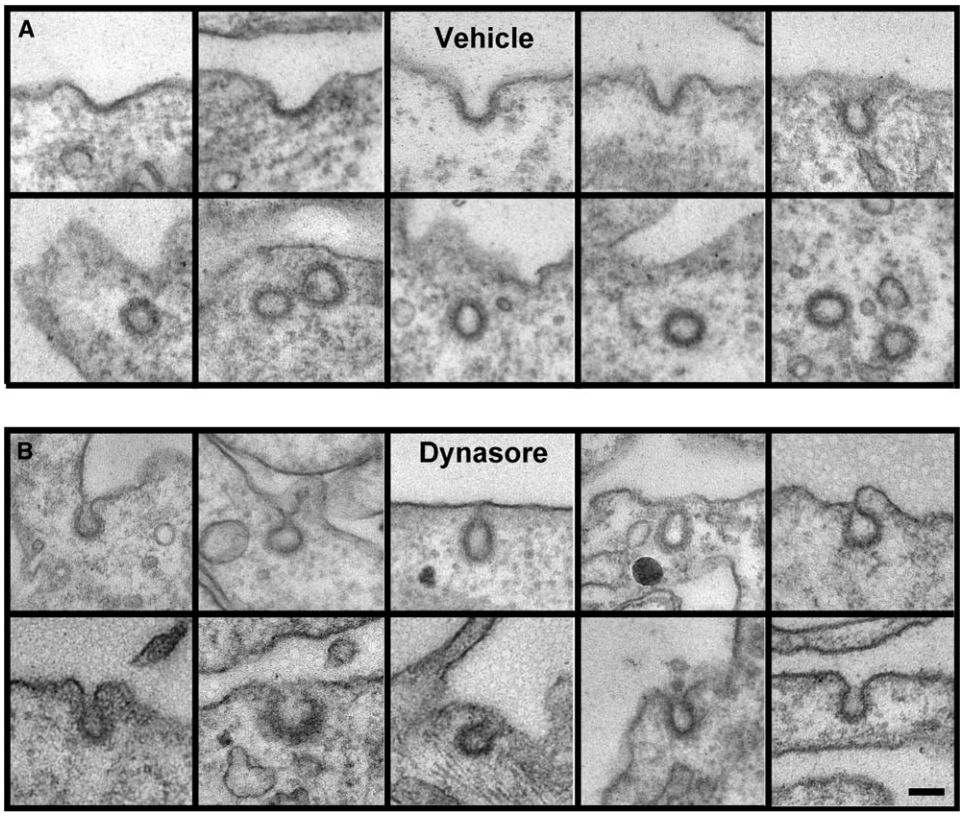

Figure 6. Stabilization by Dynasore of Clathrin-Coated Pits at Early and Late Stages of Formation

(A and B) Representative electron micrographs of membrane invaginations decorated with the bristle cytosolic layer characteristic of clathrin coats obtained from BSC1 cells in the (A) absence or (B) presence of dynasore. The cells were exposed to DMSO (vehicle) or 80 μM dynasore for 10 min before fixation and processing for electron microscopy. The scale bar is 100 nm.

colocalizes with spots containing AP-2 (Figure 4A, vehicle) or clathrin (Figure S4A) (Damke et al., 1994; Ehrlich et al., 2004; Merrifield et al., 2002), visualized here by the fluorescence of σ2-adaptin-EGFP (or EGFP-LCa) and by labeling with an antibody specific for dynamin2. Dynamin also colocalizes with AP-2 (Figure 4A, dynasore) or clathrin spots (Figure S4A) in cells treated for 45 min with 80 μM dynasore. In these experiments, we observed that there was less AP-2 or clathrin per spot, suggesting that exposure to dynasore had blocked the completion of pit formation at various stages. As explained below, this turns out to be the case. After extended treatment with dynasore, there was also an increase in the overall number of dynamin-containing spots with or without AP-2 or clathrin.

We have shown in BSC1 cells stably expressing σ2-adaptin-EGFP that the endocytic coats containing AP-2 appear and disappear and have life spans ranging between 20 and 60 s (see the kymograph in Figure 4B, vehicle; see Movie S1) (Ehrlich et al., 2004). In contrast, upon incubation for 40 min with 80 μM dynasore, the AP-2 coats become stable for long periods and remain locked at their starting positions on the membrane (note the long tracks in the kymograph for Figure 4B, dynasore; see Figure S4B for clathrin; Movie S2). This observation suggests that dynasore blocks the completion of coat assembly and therefore uncoating, presumably because GTP bound dynamin accumulates in the coated pit. These inhibitory effects are reversible upon removal of dynasore. The rapid cycle of AP-2 coat assembly and uncoating had recovered completely in cells imaged 15 min after initiation of the washout period (Figure 4B, after washout; Movie S3). The same reversible blockage was observed with clathrin coats labeled by expression of EGFP-LCa (Figure S4B).

Results from fluorescent recovery after photobleaching (FRAP) experiments (Figures 4C and 4D) confirmed the absence of newly formed coated pits in cells treated for 40–45 min with dynasore (compare the appearance of new pits in cells treated only with vehicle). It also showed that the coat components were locked within the assembled structures, as there was no detectable exchange of AP-2 (Figures 4C and 4D) or of clathrin (Figures S4C and S4D) between the coats and the cytosol in cells treated with dynasore.

Kinetics of Action of Dynasore on Coated Vesicle Formation

How rapidly does dynasore act? To answer this question, we monitored the effect of dynasore on the kinetics of coat formation for plasma membrane pits labeled with σ2-adaptin-EGFP (from AP-2) (Ehrlich et al., 2004) and imaged every 4 s starting 30 s after the addition of 80 μM dynasore (Movie S4). We identified newly formed (diffraction limited) pits and scored their frequency of appearance (Figure 5A, initiation). It took about 3–4 min to reduce by half the number of new pits that formed. We also determined as follows the time course

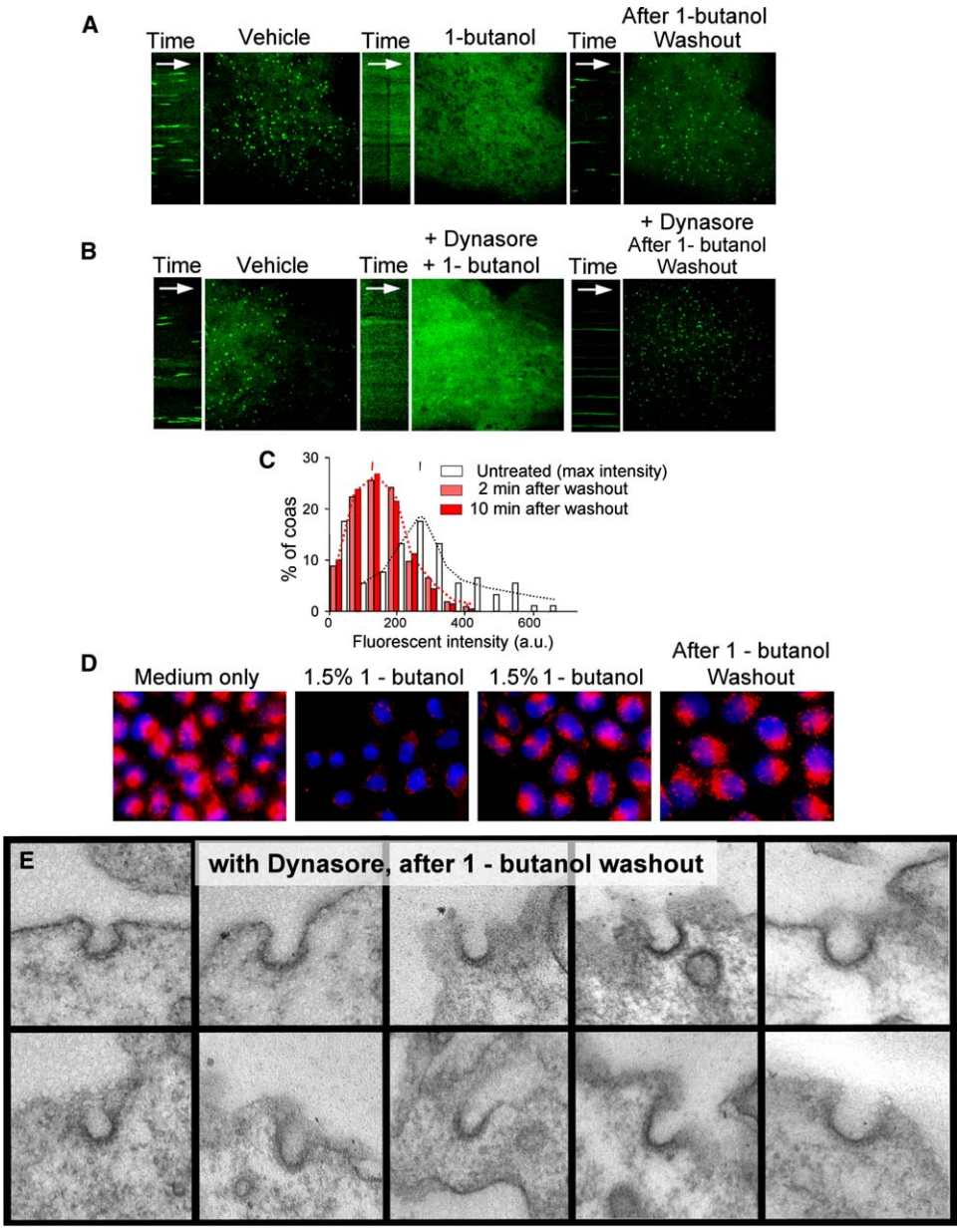

Figure 7. Accumulation of ∪-Shaped Coated Structures by Dynasore Treatment during the Synchronized Formation of New Coats upon Removal of 1-Butanol

(A) Live-cell fluorescence imaging acquired from the bottom surface of BSC1 cells stably expressing σ2-EGFP in the absence of dynasore. A control time-lapse series was collected for 2 min at 37ºC in the absence of 1-butanol (medium only). A similar time-lapse series was then collected 1 min after the addition of 1.2% v/v 1-butanol (1-butanol). Finally, a third time-lapse series was collected 2 min after removal of the 1-butanol (after 1-butanol washout).

(B) Live-cell fluorescence imaging acquired from the bottom surface of BSC1 cells stably expressing σ2-EGFP in the presence of 80 μM dynasore. A control time-lapse series was collected for 2 min at 37ºC in the absence of 1-butanol and the presence of 1% DMSO (medium only). A similar time-lapse series was then collected 20 min after the sequential addition of 1.2% v/v 1-butanol for 2 min, followed by 1.2% v/v 1-butanol together with 80 μM dynasore for an additional 20 min (+ dynasore + 1-butanol). Finally, a third time-lapse series was collected 1 min after removal of 1-butanol but still in the presence of dynasore (+ dynasore after 1-butanol washout). Each still image corresponds to a frame acquired after 2 min of any given time-lapse series, while the kymographs represents the complete time-lapse series obtained with the spinning disk confocal configuration (1 s exposures, acquired every 4 s). The data are representative of the experiment done in triplicate.

(C) Effect of dynasore on the distribution of fluorescence intensities of σ2-EGFP-containing spots after removal of 1-butanol. The histogram distribution compares the maximum fluorescence intensity of AP-2 spots just prior to their uncoating in cells not exposed to 1.2% v/v 1-butanol and dynasore (white, n = 95); in the presence of 80 μM dynasore, the fluorescence intensity was reached by AP-2 spots 2 min (pink, n = 215 spots) or 10 min (red, n = 205) after removal of 1-butanol.

(D) HeLa cells were incubated overnight in DMEM supplemented with 5% fetal bovine serum and were allowed to reach 50% confluency. Before addition of fluorescently labeled Cy3-transferrin (red) for 5 min at 37ºC, the cells were rinsed rapidly three times with the indicated four conditions and were then incubated in medium only; incubated for 1 min with 1.5% v/v 1-butanol, 1 min with 1.5% v/v t-butanol, or 1 min with 1.5% v/v 1-butanol, followed by a washout period of 5 min. The cells were acid washed before fixation to remove transferrin still bound at the cell surface. The nucleus is stained with Hoechst dye (blue).

under which dynasore inhibited uncoating. We measured the average maximum intensity of AP-2 fluorescence reached by coated pits before addition of the compound. This value represents the fluorescence of a completed pit about to pinch off (Ehrlich et al., 2004). After addition of dynasore, we followed the fate of all coated pits that reached this intensity. It took less than 1 min to reduce by half the number of such pits that were uncoated, as scored by the abrupt disappearance of AP-2 fluorescence; most initiations and uncoatings ceased 6.5 min after addition of dynasore, resulting in stable structures (Movie S5). Because the rates at which coats appear and disappear were affected differently, the total number of AP-2-containing spots increased (Figure 5B), reaching a plateau 6.5 min after the addition of dynasore (Figure 5C). Presumably, the reduction in the number of newly formed coats reflects the reduction in the amount of available free coat components. These observations indicate that access of dynasore to cells occurs quickly (less than 1 min), and that the uncoating step (and scission) is particularly sensitive to inhibition of dynamin GTP hydrolysis.

Dual Function of Dynamin during Clathrin-Mediated Endocytosis

Several lines of evidence suggest that aspects of coat formation other than pinching and uncoating also depend on dynamin's function. Dynamin is recruited even at early stages by the coat into an assembling pit (Damke et al., 2001; Ehrlich et al., 2004; Merrifield et al., 2002; Rappoport and Simon, 2003). Moreover, expression of the dominant-negative mutant dynaminK44A or depletion of wild-type dynamin (by immunoisolation) in a broken cell system leads to the accumulation of coated pits with openings that are accessible to large probes such as avidin (Damke et al., 1994, 1995b) or transferrin (Miwako et al., 2003). To investigate whether interference with the GTP hydrolysis cycle of dynamin by dynasore might affect coat formation at intermediate stages of assembly, we analyzed the structures that accumulate in cells treated with dynasore. The distribution of fluorescence intensities for all AP-2 spots recorded in a single frame represents the size distribution of the pits at all stages of their growth, while the maximum intensity attained immediately before disappearance recorded during the time-lapse series represents the coated vesicle after scission and before uncoating (Ehrlich et al., 2004). We compared the profiles obtained during the time lapse in the absence of dynasore (Figure 5D, vehicle/maximum intensity) or from single frames after incubation with 80 μM dynasore for 10 min (Figure 5D, dynasore), time at which coats no longer appear or disappear. After treatment with dynasore, we observed the same shift in the distribution to lower fluorescence intensities together with the appearance of a distinct fluorescent peak at an intensity lower than the peak value determined in the absence of dynasore. The intensity of this new peak corresponds to approximately one-half the number of AP-2 or clathrin molecules present in coated vesicles of untreated cells, as determined by the maximum fluorescence intensity recorded immediately prior to uncoating.

To correlate the live-cell imaging analysis with the structural intermediates generated by treatment with dynasore, we used electron microscopy to image the dorsal surface of cells attached to glass coverslips. Representative images from control cells (Figure 6A, vehicle) show a broad distribution of coated profiles corresponding to coated pits at all stages of invagination from the plasma membrane (top panel) in addition to complete circular profiles probably representing fully formed coated vesicles (bottom panel) (for quantification, see Figure S6). In contrast, the images obtained from cells treated with dynasore (Figure 6B, dynasore) show a large number of coated pits at partial stages of late assembly that remain linked to the plasma membrane by either narrow (top panel) or wide necks (bottom panel); the absence of long tubules decorated at their end by clathrin coats was conspicuous. Thus, these observations are consistent with a dual role of dynamin—one during the growing phase of the coat, and another for coated pit scission.

As coats still form during the first minutes of cell exposure to dynasore, it is possible that the block in coat growth represents an indirect effect due to a gradual loss of free coat components required for coat assembly. To rule out this possibility, we took advantage of the new observation (M.E., unpublished data) that exposure to 1.2% v/v 1-butanol results in a very rapid (<1 min) disappearance of all AP-2 (Figure 7A, 1-butanol and Movie S6) and clathrin coats (Figure S5) with a concomitant blockage in transferrin uptake (Figure 7C, 1.5% 1-butanol). Removal of 1-butanol leads to the synchronous appearance of newly formed coated pits and coated vesicles displaying dynamic assembly properties similar to those in untreated cells (Figure 7A, after 1-butanol washout; Movie S7), and it also leads to complete recovery of transferrin uptake (Figure 7C, after 1-butanol washout). We treated cells with dynasore after the onset of the 1-butanol-induced loss of coats (Figure 7A, + dynasore + 1-butanol), and we then removed the 1-butanol but left dynasore in the medium (Figure 7A, + dynasore after 1-butanol washout; Movie S8). Reversal of 1-butanol blockade (in the presence of dynasore) led to a synchronous wave of coat formation and allowed us to capture assembly intermediates; the fluorescence intensity of the new AP-2 spots was weaker than fully formed pits (Figure 7B), and they also remained locked at their starting positions (Movie S9). The morphological data depicted in Figure 7D (for quantification, see Figure S6) are representative of the coated pits profiles lining the plasma membrane of cells continuously exposed to 80 μM dynasore, imaged 3 min after the initiation of the washout of 1.2% 1-butanol. Most of the coated pits display characteristic ∪-like shapes, representing intermediate structures that have reached ~50% completion and that remain linked by broad

(E) BSC1 cells were briefly treated for 2 min with 1.2% v/v 1-butanol (to remove coated pits), were then treated with 1.2% v/v 1-butanol and 80 μM dynasore for 10 min, and were finally transferred for 2 min to 80 μM dynasore only. The electron micrographs are representative of coated structures observed along the plasma membrane of more than ten cells fixed and processed for electron microscopy at the end of the incubation. Very few fully formed coated pits could be found at the end of the washout period performed in the presence of dynasore (Figure S6).

necks to the plasma membrane. These images suggest that coated pits forming from an early stage encounter an assembly barrier at a point that corresponds to a relatively sharp bend in the membrane at the lip of the partially formed pit. We suggest that these intermediates are the same as the ∪-shape pits observed in cells treated only with dynasore (Figure 6B). We could only find a few images corresponding to completely formed coated pits still linked by narrow necks to the plasma membrane. The morphological data presented here can explain the live-cell imaging results, which show a clear shift to weaker fluorescent signals and the appearance of a pronounced peak of half-maximal intensity in the profile of reappearing AP-2 spots, imaged at the cell surface in the presence of dynasore after the removal of 1-butanol (Figure 7B). We believe that the coated pits within this satellite peak are the ∪-shaped invaginations that accumulate when dynasore is present. We note that the fluorescence intensity and the kinetics of formation of pits and vesicles after removal of 1-butanol were the same as in the control cells, showing that 1-butanol did not lead to long-term changes in the clathrin pathway.

Discussion

We have identified and characterized a fast-acting, cell-permeable, small-molecule dynasore that inhibits the dynamin GTPase. The experiments we report illustrate the usefulness of rapidly acting small molecules in analyzing the dynamics of membrane traffic. The mutants that have been instrumental for essentially all studies to date of dynamin function in vivo restrict accessible time constants to the range of hours to days. The effects of dynasore are evident within 1–2 min of treatment, and they are presumably limited by diffusion of the molecule to the coated pits on which it acts. The effects on a particular coated pit are presumably very rapid once the local concentration of dynasore has reached a suitable level, and they appear to be strong enough to trap assembly intermediates.

Using dynasore, we have detected two intermediates in coated vesicle formation that accumulate after a rapid shut-off of dynamin GTP hydrolysis. One of these intermediates, similar to structures frequently described in studies of dynamin temperature-sensitive mutants, is a fully formed (or nearly fully formed) coat surrounding a vesicle still connected to the cell membrane by a narrow neck. The other is an approximately hemispherical pit in the membrane that has a roughly half-formed coat. These two structures appear to represent distinct stages in coated vesicle formation, as only the latter accumulates when coated pit formation has been synchronized by application and removal of 1-butanol in the presence of the dynamin inhibitor, whereas both appear when the inhibitor is added to cells making coated pits asynchronously. The two may correspond to steps in coated vesicle assembly at which the necessary membrane distortion provides a barrier that dynamin must help overcome—the beginnings of a constriction in the growing structure and the final pinching off of a fully constricted neck. Evidence for these two intermediates comes from complementary observations with fluorescence microscopy of live cells and electron microscopy of thin sections.

The observations and conclusions described in this paper do not yet distinguish between mechanochemical and regulatory models for dynamin function. Collar formation could accelerate constriction; further conformational change could assist pinching. Recruitment of lipid-modifying factors could assist either step. While most experiments have been interpreted in terms of the pinching step, there have been hints that dynamin can act earlier. This notion evolved first from in vitro biochemical observations on perforated cells, which showed partial closure of pits under conditions of dynamin depletion (Simpson et al., 1999). More recently, the properties of the *Drosophila shibire*^{ts2} mutation and of its allelic suppressor, *sushi*^{ts2}, have led to an explicit two-step model (Narayanan et al., 2005). *shibirei*^{ts2} is partially defective in GTP binding, while two of the *sushi* mutants display an impaired GAP activity due to single amino acid substitutions toward the C-terminal end of the GED. As neither of the mammalian equivalents of these dynamin mutants is impaired in their self-assembly properties in vitro, they appear to separate dynamin assembly from GTPase stimulation. The *sushi* mutants presumably remain in the GTP state for an extended period, thus counterbalancing the lower GTP affinity. It has been suggested that GTPase activity depending on dynamin assembly might be required after collar formation, while an assembly-independent GTPase might function at a precollar stage. The morphological correlates of these effects have not yet been analyzed.

Our results also favor a dual role model and provide direct physical evidence for the stages at which dynamin functions. When a growing clathrin lattice has reached a ∪-shaped profile, dynamin appears to be necessary to counterbalance tension from the acute change in curvature at the edge of the coat. This is a precollar stage. When the coat has fully formed, acquiring an O-shaped profile, the neck has a complete dynamin collar, which may then work directly or indirectly to disconnect the budding vesicle from the parent membrane.

Experimental Procedures

Proteins

Full-length human dynamin1 was expressed in insect cells, purified by ionic exchange chromatography, and stored in 20% glycerol at −80ºC until use. Truncated N-terminally His-tagged human dynamin2 lacking its C-terminal proline-rich domain was expressed in *E. coli* and was purified with Ni-NTA chromatography. His-tagged Human MxA (Richter et al., 1995), GST-Cdc42 and p50-RhoGAP (plasmids provided by G. Kochs and O. Haller [University Freiburg, Germany], R. Cerione [Cornell University, NY], and A. Hall [University College London, London, UK]), GST-Grb2, and GST-Dyn2-GTPase were all expressed in *E. coli* and were purified with Ni-NTA or gluthathione-Sepharose chromatography, as appropriate.

Library Screen

Addition of GST-Grb2 (containing its two SH3 domains) to full-length dynamin stimulates in vitro the GTPase activity of dynamin (Barylko et al., 1998). We used this mixture to screen for interfering small molecules of dynamin-mediated GTP hydrolysis by using a 384-well format. The assay is based on the change of spectral characteristics of malachite green in the presence of free PO_4 ions (Cogan et al., 1999; Maehama et al., 2000). A fresh solution containing 0.324 mM malachite green, 0.0426% Triton X-100, 16.61 mM ammonium molybdate, and 1.246 M H_2SO_4 was prepared on the day of use. After

standing for ~2 hr at room temperature, the reagent changes from dark brown to a golden yellow and is ready for use. The screen was started by mixing 100 nM purified full-length human dynamin1 (expressed in insect cells) with 2 μM GST-Grb2 (expressed in *E. coli*) in a total volume of 30 μl containing 50 mM Tris (pH 7.5), 3 mM $MgCl_2$, 100 mM KCl, 0.2 mM EGTA. The mixture was dispensed in 384-well plates containing an optically clear bottom (Krackeler Scientific, Inc., Albany); four columns were used for controls (DMSO without dynamin, Grb2, or GTP). Approximately 100 nl library compounds (~10 mM dissolved in DMSO) was robotically pin-transferred to attain final concentrations ranging between 20 and 50 μM, depending on the molecular weights of the compounds. The reaction was started by adding ~300 nl GTP (final concentration of 200 μM), followed by a 30 min incubation at 20ºC–24ºC, and ended by addition of 50 μl malachite green. After another 15 min incubation at room temperature, the plates were placed on a plate reader (Perkin Elmer, Shelton, CT), and absorbance was determined at 650 nm. The screen was done by using a 16,320-compound library (DiversSet E; Chembridge, San Diego).

GTPase Activity

GTPase activity was measured by using a radioactive charcoal-based assay (Rasmussen et al., 1998). Briefly, proteins (dynamin, human Drp1 [provided by J. Nunnari, University of California, Davis], human MxA, GST-Cdc42 with or without its GAP p50-RhoGAP) at the indicated concentrations were incubated in 10 mM Tris (pH 7.2), 2 mM $MgCl_2$, and 20 μM $GTP\gamma P^{32}$ (2000 dpm/pmol) alone or, when appropriate, with lipid nanotubes (Stowell et al., 1999) for the indicated times and temperatures; the final NaCl concentration was 150 mM NaCl for the high-salt condition and between 10 and 20 mM for the low-salt conditions depending on the protein concentration in the stock solution. GTP hydrolysis was ended by transferring 10 μl aliquots of the reaction into a 500 μl slurry containing acid-washed charcoal, followed by a 10 min centrifugation (20000 × g, 4ºC) and final counting of the liberated $P^{32}O_4$ contained in 250 μl supernatant. The K_m and V values were obtained by using a Lineweaver-Burk linear transformation (1/V against 1/[s]) so that the intercept on the x and y axes corresponds to $-1/K_m$ and 1/V.

Cell Imaging

Live-cell fluorescent images were acquired at 37ºC by using a spinning disk confocal head attached to an inverted microscope (200M Zeiss Co.) under control of Slide Book 4 (Intelligent Imaging Innovations, Inc.) and were processed as described (Ehrlich et al., 2004). Most of the live-cell imaging experiments were done with BSC1 cells stably expressing σ2-EGFP or EGFP-LCa (Ehrlich et al., 2004). The effects of dynasore on the assembly of clathrin coats was also followed in HeLa and astrocytes cells transiently expressing EGFP-LCa. Cells were fixed with formaldehyde and processed for fluorescence microscopy (Ehrlich et al., 2004). Electron microscopy was done with HeLa cells grown on plastic coverslips after they were fixed with 2.5% glutaraldehyde/2% PFA in 0.1 M cacodylate buffer (pH 7.4) for 2 hr at room temperature. Cells were then processed for thin-section electron microscopy after epon resin embedding and osmium contrast enhancement (Massol et al., 2005). The micrographs were acquired digitally with a FEI Tecnai Spirit microscope (FEI Company) at a direct magnification of 13,000.

Supplemental Data

Supplemental Data include Seven Figures and Nine Movies and are available at http://www.developmentalcell.com/cgi/content/full/10/6/839/DC1/.

Acknowledgments

We thank W. Boll, S. Saffarian, M. Ma, and all the other members of our laboratory for their generous help and advice. We also thank the members of the Institute of Chemistry and Cell Biology, Harvard Medical School for help during the screening stage, and B. Fendly, R. Cerione, P. Chavrier, T. Dubois, A. Hall, O. Haller, G. Kochs, and J. Nunnari for kindly supplying cDNA constructs, protein, and the monoclonal antibody 13A9. We thank S.C. Harrison for inventing the term dynasore and suggesting its use. We acknowledge the generous support of the Perkin Fund to purchase part of the imaging equipment used here for live-cell imaging. M.E. was a Dorot Fellow with support from the Fulbright Foundation. E.B. is supported by a European Molecular Biology Organization long-term fellowship. This work was supported by National Institutes of Health GM62566-05, GM03548, and GM075252 (T.K).

Received: January 19, 2006
Revised: March 22, 2006
Accepted: April 3, 2006
Published: June 5, 2006

References

Abazeed, M.E., Blanchette, J.M., and Fuller, R.S. (2005). Cell-free transport from the trans-golgi network to late endosome requires factors involved in formation and consumption of clathrin-coated vesicles. J. Biol. Chem. *280*, 4442–4450. Published online November 30, 2004. 10.1074/jbc.M412553200.

Altschuler, Y., Barbas, S.M., Terlecky, L.J., Tang, K., Hardy, S., Mostov, K.E., and Schmid, S.L. (1998). Redundant and distinct functions for dynamin-1 and dynamin-2 isoforms. J. Cell Biol. *143*, 1871–1881.

Barylko, B., Binns, D., Lin, K.M., Atkinson, M.A., Jameson, D.M., Yin, H.L., and Albanesi, J.P. (1998). Synergistic activation of dynamin GTPase by Grb2 and phosphoinositides. J. Biol. Chem. *273*, 3791–3797.

Cao, H., Weller, S., Orth, J.D., Chen, J., Huang, B., Chen, J.L., Stamnes, M., and McNiven, M.A. (2005). Actin and Arf1-dependent recruitment of a cortactin-dynamin complex to the Golgi regulates post-Golgi transport. Nat. Cell Biol. *7*, 483–492. Published online April 10, 2005. 10.1038/ncb1246.

Chen, Y.J., Zhang, P., Egelman, E.H., and Hinshaw, J.E. (2004). The stalk region of dynamin drives the constriction of dynamin tubes. Nat. Struct. Mol. Biol. *11*, 574–575. Published online May 9, 2004. 10.1038/nsmb762.

Cogan, E.B., Birrell, G.B., and Griffith, O.H. (1999). A robotics-based automated assay for inorganic and organic phosphates. Anal. Biochem. *271*, 29–35.

Damke, H., Baba, T., Warnock, D.E., and Schmid, S.L. (1994). Induction of mutant dynamin specifically blocks endocytic coated vesicle formation. J. Cell Biol. *127*, 915–934.

Damke, H., Baba, T., van der Bliek, A.M., and Schmid, S.L. (1995a). Clathrin-independent pinocytosis is induced in cells overexpressing a temperature-sensitive mutant of dynamin. J. Cell Biol. *131*, 69–80.

Damke, H., Gossen, M., Freundlieb, S., Bujard, H., and Schmid, S.L. (1995b). Tightly regulated and inducible expression of dominant interfering dynamin mutant in stably transformed HeLa cells. Methods Enzymol. *257*, 209–220.

Damke, H., Binns, D.D., Ueda, H., Schmid, S.L., and Baba, T. (2001). Dynamin GTPase domain mutants block endocytic vesicle formation at morphologically distinct stages. Mol. Biol. Cell *12*, 2578–2589.

Danino, D., and Hinshaw, J.E. (2001). Dynamin family of mechanoenzymes. Curr. Opin. Cell Biol. *13*, 454–460.

Danino, D., Moon, K.H., and Hinshaw, J.E. (2004). Rapid constriction of lipid bilayers by the mechanochemical enzyme dynamin. J. Struct. Biol. *147*, 259–267.

Eccleston, J.F., Binns, D.D., Davis, C.T., Albanesi, J.P., and Jameson, D.M. (2002). Oligomerization and kinetic mechanism of the dynamin GTPase. Eur. Biophys. J. *31*, 275–282.

Ehrlich, M., Boll, W., Van Oijen, A., Hariharan, R., Chandran, K., Nibert, M.L., and Kirchhausen, T. (2004). Endocytosis by random initiation and stabilization of clathrin-coated pits. Cell *118*, 591–605.

Ezratty, E.J., Partridge, M.A., and Gundersen, G.G. (2005). Microtubule-induced focal adhesion disassembly is mediated by dynamin and focal adhesion kinase. Nat. Cell Biol. *7*, 581–590. Published online May 15, 2005. 10.1038/ncb1262.

Gout, I., Dhand, R., Hiles, I.D., Fry, M.J., Panayotou, G., Das, P., Truong, O., Totty, N.F., Hsuan, J., Booker, G.W., et al. (1993). The GTPase dynamin binds to and is activated by a subset of SH3 domains. Cell *75*, 25–36.

Hanover, J.A., Willingham, M.C., and Pastan, I. (1984). Kinetics of transit of transferrin and epidermal growth factor through clathrin-coated membranes. Cell *39*, 283–293.

Henley, J.R., Krueger, E.W.A., Oswald, B.J., and McNiven, M.A. (1998). Dynamin-mediated internalization of caveolae. J. Cell Biol. *141*, 85–99.

Hill, E., van der Kaay, J., Downes, C.P., and Smythe, E. (2001). The role of dynamin and its binding partners in coated pit invagination and scission. J. Cell Biol. *152*, 309–323.

Horisberger, M.A. (1992). Interferon-induced human protein MxA is a GTPase which binds transiently to cellular proteins. J. Virol. *66*, 4705–4709.

Jiang, X., and Sorkin, A. (2003). Epidermal growth factor receptor internalization through clathrin-coated pits requires Cbl RING finger and proline-rich domains but not receptor polyubiquitylation. Traffic *4*, 529–543.

Kelly, R.B. (1999). New twists for dynamin. Nat. Cell Biol. *1*, E8–E9.

Kirchhausen, T. (1999). Cell biology. Boa constrictor or rattlesnake? Nature *398*, 470–471.

Kochs, G., Haener, M., Aebi, U., and Haller, O. (2002). Self-assembly of human MxA GTPase into highly ordered dynamin-like oligomers. J. Biol. Chem. *277*, 14172–14176.

Koenig, J.H., and Ikeda, K. (1989). Disappearance and reformation of synaptic vesicle membrane upon transmitter release observed under reversible blockage of membrane retrieval. J. Neurosci. *9*, 3844–3860.

Kosaka, T., and Ikeda, K. (1983). Reversible blockage of membrane retrieval and endocytosis in the garland cell of the temperature-sensitive mutant of *Drosophila melanogaster*, shibirets1. J. Cell Biol. *97*, 499–507.

Lancaster, C.A., Taylor-Harris, P.M., Self, A.J., Brill, S., van Erp, H.E., and Hall, A. (1994). Characterization of rhoGAP. A GTPase-activating protein for rho-related small GTPases. J. Biol. Chem. *269*, 1137–1142.

Maehama, T., Taylor, G.S., Slama, J.T., and Dixon, J.E. (2000). A sensitive assay for phosphoinositide phosphatases. Anal. Biochem. *279*, 248–250.

Marks, B., Stowell, M.H.B., Vallis, Y., Mills, I.G., Gibson, A., Hopkins, C.R., and McMahon, H.T. (2001). GTPase activity of dynamin and resulting conformation change are essential for endocytosis. Nature *410*, 231–235.

Massol, R.H., Larsen, J.E., Fujinaga, Y., Lencer, W.I., and Kirchhausen, T. (2004). Cholera toxin toxicity does not require functional Arf6- and dynamin-dependent endocytic pathways. Mol. Biol. Cell *15*, 3631–3641.

Massol, R.H., Larsen, J.E., and Kirchhausen, T. (2005). Possible role of deep tubular invaginations of the plasma membrane in MHC-I trafficking. Exp. Cell Res. *306*, 142–149.

McNiven, M.A. (1998). Dynamin: a molecular motor with pinchase action. Cell *94*, 151–154.

Merrifield, C.J., Feldman, M.E., Wan, L., and Almers, W. (2002). Imaging actin and dynamin recruitment during invagination of single clathrin-coated pits. Nat. Cell Biol. *4*, 691–698.

Miwako, I., Schroter, T., and Schmid, S.L. (2003). Clathrin- and dynamin-dependent coated vesicle formation from isolated plasma membranes. Traffic *4*, 376–389.

Nabi, I.R., and Le, P.U. (2003). Caveolae/raft-dependent endocytosis. J. Cell Biol. *161*, 673–677.

Narayanan, R., Leonard, M., Song, B.D., Schmid, S.L., and Ramaswami, M. (2005). An internal GAP domain negatively regulates presynaptic dynamin in vivo: a two-step model for dynamin function. J. Cell Biol. *169*, 117–126.

Nichols, B. (2003). Caveosomes and endocytosis of lipid rafts. J. Cell Sci. *116*, 4707–4714.

Oh, P., McIntosh, D.P., and Schnitzer, J.E. (1998). Dynamin at the neck of caveolae mediates their budding to form transport vesicles by GTP-driven fission from the plasma membrane of endothelium. J. Cell Biol. *141*, 101–114.

Orth, J.D., and McNiven, M.A. (2003). Dynamin at the actin-membrane interface. Curr. Opin. Cell Biol. *15*, 31–39.

Praefcke, G.J., McMahon, H.T., Engqvist-Goldstein, A.E., Drubin, D.G., Lang, T., Korolchuk, V., Banting, G., Song, B.D., Schmid, S.L., Wiejak, J., et al. (2004). The dynamin superfamily: universal membrane tubulation and fission molecules? Nat. Rev. Mol. Cell Biol. *5*, 133–147.

Rappoport, J.Z., and Simon, S.M. (2003). Real-time analysis of clathrin-mediated endocytosis during cell migration. J. Cell Sci. *116*, 847–855.

Rasmussen, R.K., Rusak, J., Price, G., Robinson, P.J., Simpson, R.J., and Dorow, D.S. (1998). Mixed-lineage kinase 2–SH3 domain binds dynamin and greatly enhances activation of GTPase by phospholipid. Biochem. J. *335*, 119–124.

Richter, M.F., Schwemmle, M., Herrmann, C., Wittinghofer, A., and Staeheli, P. (1995). Interferon-induced MxA protein. GTP binding and GTP hydrolysis properties. J. Biol. Chem. *270*, 13512–13517.

Schlunck, G., Damke, H., Kiosses, W.B., Rusk, N., Symons, M.H., Waterman-Storer, C.M., Schmid, S.L., and Schwartz, M.A. (2004). Modulation of Rac localization and function by dynamin. Mol. Biol. Cell *15*, 256–267. Published online November 14, 2003. 10.1091/mbc.E03-01-0019.

Sever, S. (2002). Dynamin and endocytosis. Curr. Opin. Cell Biol. *14*, 463–467.

Sever, S., Damke, H., and Schmid, S.L. (2000a). Dynamin:GTP controls the formation of constricted coated pits, the rate limiting step in clathrin-mediated endocytosis. J. Cell Biol. *150*, 1137–1148.

Sever, S., Damke, H., and Schmmid, S.L. (2000b). Garrotes, springs, ratches and whips: putting dynamin models to test. Traffic *1*, 385–392.

Simpson, F., Hussain, N.K., Qualmann, B., Kelly, R.B., Kay, B.K., McPherson, P.S., and Schmid, S.L. (1999). SH3-domain-containing proteins function at distinct steps in clathrin-coated vesicle formation. Nat. Cell Biol. *1*, 119–124.

Song, B.D., and Schmid, S.L. (2003). A molecular motor or a regulator? Dynamin's in a class of its own. Biochemistry *42*, 1369–1376.

Song, B.D., Leonard, M., and Schmid, S.L. (2004). Dynamin GTPase domain mutants that differentially affect GTP binding, GTP hydrolysis, and clathrin-mediated endocytosis. J. Biol. Chem. *279*, 40431–40436. Published online July 19, 2004. 10.1074/jbc.M407007200.

Stowell, M.H., Marks, B., Wigge, P., and McMahon, H.T. (1999). Nucleotide-dependent conformational changes in dynamin: evidence for a mechanochemical molecular spring. Nat. Cell Biol. *1*, 27–32.

Sweitzer, S.M., and Hinshaw, J.E. (1998). Dynamin undergoes a GTP-dependent conformational change causing vesiculation. Cell *93*, 1021–1029.

Torgersen, M.L., Skretting, G., van Deurs, B., and Sandvig, K. (2001). Internalization of cholera toxin by different endocytic mechanisms. J. Cell Sci. *114*, 3737–3747.

Yang, W.N., and Cerione, R.A. (1999). Endocytosis: is dynamin a 'blue collar' or 'white collar' worker? Curr. Biol. *9*, R511–R514.

Zhang, P.J., and Hinshaw, J.E. (2001). Three-dimensional reconstruction of dynamin in the constricted state. Nat. Cell Biol. *3*, 922–926.